A Comparative Study of Macroporous Metal Oxides Synthesized via a Unified Approach

Sikander H. Hakim and Brent H. Shanks*

Department of Chemical and Biological Engineering, Iowa State University, 2119 Sweeney Hall, Ames, Iowa, 50011

Received June 20, 2008. Revised Manuscript Received March 19, 2009

A variety of macroporous metal oxides was synthesized via a spontaneous self-assembly process in aqueous solution starting from organic alkoxide precursors under a common set of conditions to present a consistent set of data for evaluation of macropore formation in these materials that are known to yield such structural patterns. Sol−gel-type chemistry appears to be governing the structure formation in these materials, so the influence of sol−gel parameters such as the alkyl group in the alkoxide, the central metal atom, and the pH of the reaction mixture were investigated in order to gain insight on the defining mechanism dictating the formation of these structures. The results revealed that depending upon the central metal atom or the alkyl group, the alkoxide precursors had characteristic hydrolysis and condensation rates, which, when balanced appropriately, resulted in structured macroporous pattern formation in the final materials. Powders obtained in the spontaneous self-assembly processes were found to have varying macropore sizes as well as extents of macroporosity upon adjusting standard sol−gel synthesis parameters, which control the relative rates of the hydrolysis and condensation reactions.

1. Introduction

The nanostructural design of materials is attracting increasing attention in the development of improved catalysts. Of particular interest are materials with structural hierarchy. These unique structures incorporate interconnected pores of two different length scales. The mesopores provide high surface area and the macropores render the mesopores more accessible by reducing diffusion resistance, which can limit the application of mesoporous catalytic materials. Since macropores have the potential to enhance the catalytic activity of these materials, the design of catalytic materials with incorporated macropores is of interest. Introduction of secondary macropores in mesoporous framework has been demonstrated to increase the activity of solid catalysts significantly by enhancing the diffusion to and from the active sites.[1,2] Incorporation of macroporous channels in mesoporous titania framework was also found to increase the photocatalytic activity of the catalyst by increasing the photoabsorption efficiency and efficient diffusion of gaseous molecules.[3] Besides their applications in catalysis, hierarchically structured materials have also displayed remarkable properties in separations as a stationary phase of high performance liquid chromatography (HPLC) compared to conventional particle-packed systems.[4]

A challenge is to synthesize materials with pores at two different length scales while being able to control independently the individual pore structures. A review of possible approaches has been recently provided by Yuan et al.[5] For the creation of mesopores, self-assembled molecular aggregates or supramolecular assemblies are generally employed, while for creation of macropores, appropriately sized sacrificial substances such as colloidal crystals, polymer foams, biocelluloses, emulsions, and vesicles were added during the synthesis. Synthesis approaches have also been directed toward developing routes to hierarchical materials and porous materials in general that do not involve any templating. Template-free methods such as redox cycling to produce mesopores in a regenerative process in a macroporous material[6] or selective leaching of one phase from a two-phase composite[7] have been reported. Nakanishi developed a route to obtain hierarchical materials by means of liquid−liquid phase separation induced by water-soluble polymers such as PEO to control the phase separation/gelation kinetics.[4] The phase separation driven by a repulsive interaction between the hydrophobic PEO-oligomeric complex and the hydrophilic solvent resulted in the macroporous morphology.

A simpler template-free technique, which is the focus of the current work, obtains hierarchically structured meso−macroporous or purely macroporous materials via a spontaneous self-assembly mechanism.[8,9] In this technique, highly reactive liquid metal alkoxides are allowed to hydrolyze and condense to instantaneously form a porous metal oxide network. This technique produces powder particles with

* Corresponding author. Tel: 515−294−1895. Fax: 515−294−2628. E-mail: bshanks@iastate.edu.

(1) Takahashi, R.; Sato, S.; Sodesawa, T.; Arai, K.; Yabuki, M. *J. Catal.* **2005**, *229*, 24–29.
(2) Chen, W.-H.; Zhao, Q.; Lin, H.-P.; Yang, Y.-S.; Mou, C.-Y.; Liu, S.-B. *Microporous Mesoporous Mater.* **2003**, *66*, 209–218.
(3) Wang, X.; Yu, J. C.; Ho, C.; Hou, Y.; Fu, X. *Langmuir* **2005**, *21*, 2552–2559.
(4) Nakanishi, K. *Mater. Res. Soc. Symp. Proc.* **2007**, *1007*, 51–62; Paper # 1007-S1003-1001.
(5) Yuan, Z.-Y.; Su, B.-L. *J. Mater. Chem.* **2006**, *16*, 663–677.
(6) Toberer, E. S.; Schladt, T. D.; Seshadri, R. *J. Am. Chem. Soc.* **2006**, *128*, 1462–1463.
(7) Toberer, E. S.; Seshadri, R. *Chem. Commun. (Cambridge, UK)* **2006**, *315*, 9–3165.
(8) Deng, W.; Toepke, M. W.; Shanks, B. H. *Adv. Funct. Mater.* **2003**, *13*, 61–65.
(9) Deng, W.; Shanks, B. H. *Chem. Mater.* **2005**, *17*, 3092–3100.

10.1021/cm801691g CCC: $40.75
Published on Web 04/23/2009

unique morphology in which parallel macropores (with micro/mesoporous walls in hierarchical materials) traverse through the particles. This architecture has not been reported using any of the other methods mentioned above. Very pure oxide materials can be prepared starting with just the alkoxide precursors in aqueous solutions, as opposed to other synthesis strategies where the resultant oxides are often contaminated by residual species. Additionally, since the structures can be obtained in the presence or absence of surfactants (indicating no direct surfactant role in pattern formation other than potential improved mesostructure[9,10]), either no post-treatment is required or, if present, the surfactants can be easily removed. Crystalline phases were found to be present in the products obtained using this technique in contrast to completely amorphous products obtained via templating procedures.[9,11] Some of these materials have shown higher thermal stability relative to respective surfactant-templated meso−macroporous materials.[12]

A rapid precipitation of the metal oxide/hydroxide from solution is a key to the formation of macropores. Whether or not the final macroporous material will have a framework consisting of smaller pores (micropores or mesopores) depends upon the type of metal oxide material as well as on the synthesis conditions. A spontaneously formed macroporous structure was first reported by Yoldas[13] from experiments examining the effect of hydrolysis conditions on the molecular and particulate morphology of titanium oxide particles. "Honeycomb" morphology of titania powders was reported when starting from titanium ethoxide under alkaline conditions, which contrasted with granular morphologies obtained under acidic or neutral conditions. Our group observed these macroporous structures in a one-pot synthesis of hierarchical meso−macroporous alumina starting from aluminum tri-*sec*-butoxide in the presence of a surfactant.[8] Particles were found to contain parallel arrays of macropores with mesoporous walls. Also, the synthesis of meso−macroporous zirconia in the presence of surfactant was reported by the Su group.[14] A more detailed synthesis of macroporous titania powders by a self-assembly mechanism in the absence of any surfactant has been reported by the Mann group.[15] Recently, the flexibility of the spontaneous self-assembly process has been demonstrated by extending the synthesis from hierarchically structured pure metal oxides to mixed metal oxides[5,16,17] as well as metal oxides with phosphate groups incorporated into the oxide framework[11,18,19] for potential applications as solid acid catalysts.

Depending upon the type of starting material, the spontaneous self-assembly process that gives rise to hierarchically structured materials can take place under a wide range of synthesis conditions. For example, such an assembly is possible in an aqueous acidic solution[20] using different inorganic acids or in an alkaline solution using aqueous ammonia[15] or other bases,[20] in the presence or absence of a surfactant[9,10] or a cosolvent.[8,9] Therefore, an array of individual studies has been reported that resulted in a range of purely macroporous or hierarchically structured meso−macroporous materials. While the range of synthesis approaches that have been reported provide an interesting background, the information is not easily compiled into a consolidated framework for the formation of these unique structures. Therefore, the motivation for the current work is to provide a more systematic basis for their synthesis, thereby allowing comparison of different approaches.

Although hierarchically structured meso−macroporous metal oxides have been obtained by several researchers, the understanding of the pattern formation is very limited, which has led to a range of hypotheses. Su and co-workers has proposed a mechanism where the formation of supermicelles by the coalescence of multiple micelles and interaggregate interactions was interpreted to form macropores.[14,21] In our recent paper, by means of a detailed parametric study, it was demonstrated that the pore structure at two length scales (mesopores and macropores) could be independently modified, suggesting that individual mechanisms are associated with their formation.[9] The formation of smaller mesopores appears to be governed by a nanoparticle aggregation mechanism,[9,22] but the precise underlying mechanism of the formation of macropores in these materials remains elusive. Collins et al. developed a model to explain the formation of macropores in titania synthesized with titanium alkoxides using a self-assembly process.[15] The model explains many characteristics of the formation process for all the materials in general but left several questions unanswered.[9] In view of the current limited knowledge, there is need for further work. A deeper understanding of the formation mechanism is required not only in order to understand the pattern formation but also to help in the design of materials with adjustable and well-defined macropores, which is important for the application of these materials in catalysis.

The rapidity of the formation process makes the direct visualization needed for a mechanistic study of macropore formation very difficult. However, exploring the chemistry behind the process serves as an indirect approach for identifying the defining forces for the pattern formation. Understanding the behavior of different materials producing macroporous powders, under a particular reaction environ-

(10) Leonard, A.; Su, B.-L. *Colloids Surf., A* **2007**, *300*, 129–135.
(11) Yuan, Z.-Y.; Ren, T.-Z.; Azioune, A.; Pireaux, J.-J.; Su, B.-L. *Chem. Mater.* **2006**, *18*, 1753–1767.
(12) Ren, T.-Z.; Yuan, Z.-Y.; Su, B.-L. *Chem. Commun. (Cambridge, UK)* **2004**, *273*, 0–2731.
(13) Yoldas, B. E. *J. Mater. Sci.* **1986**, *21*, 1087–1092.
(14) Yuan, Z.-Y.; Vantomme, A.; Leonard, A.; Su, B.-L. *Chem. Commun. (Cambridge, UK)* **2003**, *155*, 8–1559.
(15) Collins, A.; Carriazo, D.; Davis, S. A.; Mann, S. *Chem. Commun. (Cambridge, UK)* **2004**, *56*, 8–569.
(16) Vantomme, A.; Leonard, A.; Yuan, Z.-Y.; Su, B.-L. *Colloids Surf., A* **2007**, *300*, 70–78.
(17) Yuan, Z.-Y.; Ren, T.-Z.; Vantomme, A.; Su, B.-L. *Chem. Mater.* **2004**, *16*, 5096–5106.
(18) Ren, T.-Z.; Yuan, Z.-Y.; Azioune, A.; Pireaux, J.-J.; Su, B.-L. *Langmuir* **2006**, *22*, 3886–3894.
(19) Yuan, Z.-Y.; Ren, T.-Z.; Azioune, A.; Pireaux, J.-J.; Su, B.-L. *Catal. Today* **2005**, *105*, 647–654.
(20) Leonard, A.; Su, B.-L. *Chem. Commun. (Cambridge, UK)* **2004**, *167*, 4–1675.
(21) Blin, J.-L.; Leonard, A.; Yuan, Z.-Y.; Gigot, L.; Vantomme, A.; Cheetham, A. K.; Su, B.-L. *Angew. Chem., Int. Ed.* **2003**, *42*, 2872–2875.
(22) Hicks, R. W.; Pinnavaia, T. J. *Chem. Mater.* **2003**, *15*, 78–82.

ment, offers useful insights. The current work performs a unified synthesis of a range of macroporous metal oxides following a consistent methodology under identical conditions. This work provides a systematic comparison of these materials, which are split based on the differences between their characteristic chemistries. The majority of the results concern macropore formation, which is the focus in the current work, so only a generalized description of the mesostructure is provided.

2. Experimental Section

2.1. Synthesis. Micro/meso−macroporous materials were obtained for titanium oxide, zirconium oxide, and aluminum oxyhydroxide. The titania powders were prepared using five different alkoxide precursors: titanium ethoxide, titanium *n*-propoxide, titanium isopropoxide, titanium *n*-butoxide, and titanium *tert*-butoxide. For zirconium, two alkoxides with normal alkyl chains, zirconium propoxide and zirconium butoxide, were used, while only a single liquid alkoxide of aluminum was investigated. The liquid precursor metal alkoxides aluminum tri-*sec*-butoxide (TBOA; 97%, Aldrich), titanium ethoxide (33+%TiO_2, Acros), titanium *n*-propoxide (98%, Aldrich), titanium isopropoxide (98+%, Aldrich), titanium *n*-butoxide (99%, Acros), titanium *tert*-butoxide (Acros), zirconium propoxide (70% solution in 1-propanol, Aldrich), and zirconium butoxide (80% solution in 1-butanol, Aldrich) were used as purchased. Deionized water was used in all syntheses and the pH was adjusted using hydrochloric acid or a stock solution of aqueous ammonia (>35%).

In our earlier paper[9] that dealt in detail with the hydrodynamic conditions during the syntheses of hierarchical alumina materials, it was found that stationary medium syntheses produced powders with a high extent of macroporosity. The stationary medium for syntheses was also recommended by Collins et al. for the synthesis of macroporous titania.[15] Thus, all syntheses here were performed in stationary medium in the absence of any stirring for the sake of consistency.

In a typical synthesis, 3 mL of alkoxide was added to 30 mL of pH-adjusted aqueous solution using the method described previously.[9] For each alkoxide, the synthesis was performed at starting pH values ranging from 0.5 to 13.5. The alkoxide droplets were then introduced directly into the solution at room temperature, as the direct contact of the droplet is indispensable for obtaining the desired morphology.[9] The alkoxide was introduced in the reaction solution at a rate of about 1 mL/min in the form of 2.5 mm diameter droplets by using a syringe. Immediate reaction was observed upon introduction of the alkoxides. TBOA droplets became smaller as a result of the formed alumina particles detaching from the droplet surface. This particle detachment was not observed for titania and zirconia, where the final solid particles retained the general shape of the initial droplets. The high reactivity of alkoxides in excess water resulted in instantaneous formation of solid oxide/oxyhydroxide except for very acidic pH values such as 0.5, where the droplets hydrolyzed rapidly, yielding clear solutions for all the three materials. The mixture was then allowed to react in the mother liquor solution at room temperature for 1 h. The powder sample was retrieved by filtration and washed with DI water. It was then allowed to dry in air at ambient temperature for 12 h and at 100 °C for 5 h.

2.2. Characterization. The macropores in the resulting metal oxides were analyzed using scanning electron microscopy (SEM). Images were taken using a JSM-840 scanning electron microscope (JEOL Inc.) with gold-coated sample preparation. Morphological information such as the fraction of particles containing macropores, the extent of macroporosity in the particles, and the pore size distribution as well as surface details regarding the aggregation of particles constituting the macropore walls was obtained by collecting images at various magnifications. The macropore diameters were measured using image processing software, Quartz PCI, for a statistically sufficient number of particles in each case to determine the median macropore diameter value.

Hg porosimetry experiments were performed using a Quantachrome Corp. Poremaster 60 pore size analyzer. Low-pressure Hg-intrusion readings were obtained for a pressure range of 0−50 psi, while the high-pressure readings were obtained for the pressure range 20−10 000 psi. The preservation of the fragile oxide structures under the high-pressure Hg-intrusion conditions was a crucial issue. Since Hg porosimetry is a bulk technique, the results were obtained to compliment the results from SEM analysis, which was the primary technique for characterizing the macroporosity.

The micro/mesostructure in the sample was characterized using a Micromeritics ASAP-2020 analyzer. The specific surface area of the materials was obtained from the nitrogen adsorption−desorption isotherm at liquid nitrogen temperature by using the BET method. The pore size distribution and pore volume were calculated from the desorption branch using the BJH method. The contributions of the micropores were evaluated using *t*-plots.

X-ray diffraction patters were obtained for information regarding the crystallinity of the resultant powders. The measurements were carried out on Siemens D-500 XRD using Cu Kα radiation.

3. Results and Discussion

In the spontaneous self-assembly phenomenon, the reaction conditions lead to an instantaneous precipitation reaction, where a solid metal oxide phase is formed starting from the liquid precursor via a hydrolysis−condensation process. The self-assembly of the solid nanoparticles results in pores at two length scales. First, they organize themselves to form the macroporous structure. And, second, the interstitial voids in between these nanoparticles give rise to mesoporosity. The hierarchical structure in the current study is possible only when the self-assembly process occurs spontaneously, which will be referred to as *spontaneous self-assembly*. This process is markedly distinct from the sol−gel process, which is a controlled multistep process with each step providing an opportunity to influence structure evolution. Slowing down of the current spontaneous self-assembly would result in similar steps; however, the resulting materials from these controlled processes would not contain a parallel array of macropores. The spontaneous self-assembly process can be viewed as a limiting case of the sol−gel process, the major difference being the uncontrolled hydrolytic condensation chemistry occurring in the former. Collins et al. viewed the phenomenon as a coupling between sol−gel reactions and physical phenomena such as microphase separation.[15] The synthesis of aluminosilicates under acidic conditions also led to the formation of gelatinous precipitates that contained macropores.[10] The important sol−gel parameters that influence the structure of the final gel network are the internal parameters, such as the central metal atom of the precursor alkoxide and the alkyl group in the alkoxide, and the external parameters of water/alkoxide ratio and pH of the solution.[13,23,24]

(23) Livage, J.; Henry, M.; Sanchez, C. *Prog. Solid State Chem.* **1988**, *18*, 259–341.

Table 1. Range of Median Macropore Diameters (MMPD in μm) for Various Materials Obtained Using Different Starting Alkoxides and pH Values

	zirconium oxide		titanium oxide					
pH	$Zr(OPr^n)_4$	$Zr(OBu^n)_4$	$Ti(OEt)_4$	$Ti(OPr^i)_4$	$Ti(OPr^n)_4$	$Ti(OBu^t)_4$	$Ti(OBu^n)_4$	alumina: $Al(OBu^s)_3$
3.0			−	3.5−4.5	−	2.0−2.5	−	2.0−2.5
7.0	2.0−4.0[a]	2.2−4.0[a]	−	−	−	−	−	2.0−2.5
11.5			4.5−5.0	4.5	6.0−8.0	−	−	1.2−1.5
13.5	1.2−2.0	2.5−5.5	−	3.5	3.0−5.0	−	2.5−3.0	1.2−1.5

[a] MMPD values remained approximately within this range for starting pH values in the range of 3.0−11.5.

It is known that the chemistry occurring in the initial stages of the sol−gel process dictates the structure of the resulting gel.[25,26] The hydrolytic condensation chemistry is the key factor determining the structure of the final oxide product; consequently, investigating the ways in which it can be carefully controlled could also provide useful insight into understanding of the macroporous pattern formation. Therefore, the current work explores the influence of some of these parameters (except for the alkoxide/water ratio, since the reaction takes place in excess water) on the macroporosity in the resultant powders from the spontaneous self-assembly process.

3.1. Effect of Central Metal Atom. For very high reactivity toward hydrolysis and condensation, the central metal atom in the starting alkoxide must be highly electropositive. Such reactivity is present in alkoxides of metals like aluminum and transition metals such as titanium and zirconium. Materials synthesized from alkoxides with different central metal atoms displayed very distinct macroporous patterns that could easily be distinguished from one another. Differences in macropore sizes were also evident (Table 1). An appropriate material can be chosen for specific applications where smaller pores were obtained with aluminum or zirconium oxides, while bigger pores were found with titanium oxides. However, for a specific metal oxide material, with a careful choice of starting alkoxides and synthesis conditions, a tailored pore size can be obtained, as will be discussed under Effect of Alkyl Groups and pH.

The difference in the central metal atom was also evident in the shape and size of the particles constituting the macroporous walls. SEM revealed that the macroporous walls were composed of individual or fused spherical particle aggregates for titanium and zirconium oxides. These aggregated particles were bigger for titanium oxide (600−800 nm) than zirconium oxide (400 nm). For alumina, the finer structure in the macroporous walls was not visible under SEM but has been reported elsewhere to be made up of fibrous nanoparticles of boehmite when observed under transmission electron microscopy (TEM).[27]

The macrostructure remained intact in all of the three materials after calcination at 550 °C in flowing air. The macropores in titania and zirconia were stable after hydrothermal aging up to 100 °C in their mother liquor solution. The extent of macroporosity in alumina appeared to decrease after aging, and no macropores were observed after 100 °C aging due to increased solubility of alumina at higher temperatures; apparently, dissolution reprecipitation led to the disappearance of the macropores. Since the focus of the current work is the formation of macropores, the influence of aging on the mesostructure of the metal oxides is not discussed here.

The mico/mesostructure in the synthesized materials was analyzed using N_2 adsorption−desorption studies. A type IV isotherm with a H2 hysteresis (BDDT classification)[28] was obtained for the alumina materials (Figure 1a). The hysteresis suggested a network of ink-bottle-shaped pores. The total surface area was 260 m^2/g and the BJH pore volume was 0.36 cm^3/g. The BJH pore size distribution determined by desorption branch indicated a pore neck of size 4 nm or smaller.[29] The mesostructure was thermally stable, and there was no decrease in total surface area after calcination at 550 °C in flowing air for 5 h.

For the titania and zirconia materials, the isotherm was a combination of types I and IV, indicating the presence of both micropores and mesopores (Figures 2a, 3a). Such bimodal porosity was due to intra- and interparticle porosity.[30] The intraparticle porosity resulted in smaller pores in the micro to smaller meso region, while the interparticle porosity resulted in larger slit-shaped pores (indicated by H3 hysteresis)[28] in meso- to macropore region. The intraparticle pore sizes determined from adsorption and desorption branches were close to each other. However, the interparticle pore size could not be accurately determined due to the presence of large meso−macropores, which are outside the range of pore sizes that can be determined by nitrogen physisorption. A continuous intrusion was also observed during Hg-porosimetry analysis. Thus, the interparticle pore size ranges from 50 nm to a few hundred nanometers, as suggested by nitrogen physisorption and SEM images. The total surface area was 320 m^2/g for titania with 120 m^2/g contributed by the micropores. Upon heat treatment, the sintering of particles led to a reduction in the total surface area, and the intraparticle pore size increased from the micro to meso range (2.6 nm). The total surface area was reduced to 103 m^2/g after calcination at 500 °C and to 2.5 m^2/g after calcination at 1000 °C. As-synthesized zirconia had a total surface area of 20−60 m^2/g, which increased to 450 m^2/g after aging in mother liquor solution for 24 h at 100 °C.

(24) Yoldas, B. E. *J. Mater. Sci.* **1986**, *21*, 1080–1086.
(25) Ya, N.; Turova, E. P. T.; Kessler, V. G.; Yanovskaya, M. I. *The Chemistry of Metal Alkoxides*; Kluwer Academic Publishers: New York, 2002.
(26) Hu, M. Z. C.; Zielke, J. T.; Byers, C. H.; Lin, J. S.; Harris, M. T. *J. Mater. Sci.* **2000**, *35*, 1957–1971.
(27) Ren, T.-Z.; Yuan, Z.-Y.; Su, B.-L. *Langmuir* **2004**, *20*, 1531–1534.
(28) Sing, K. S. W.; Everett, D. H.; Haul, R. A. W.; Moscou, L.; Pierotti, R. A.; Rouquerol, J.; Siemieniewska, T. *Pure Appl. Chem.* **1985**, *57*, 603–619.
(29) Groen, J. C.; Perez-Ramirez, J. *Appl. Catal., A* **2004**, *268*, 121–125.
(30) Yu, J.; Yu, J. C.; Leung, M. K. P.; Ho, W.; Cheng, B.; Zhao, X.; Zhao, J. *J. Catal.* **2003**, *217*, 69–78.

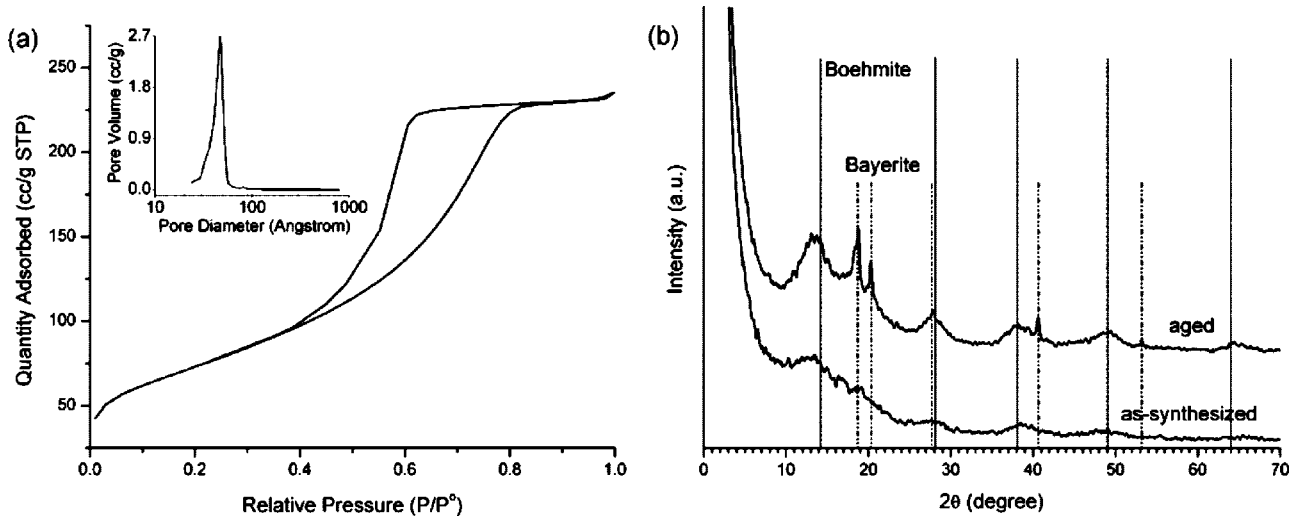

Figure 1. (a) N_2 adsorption−desorption isotherm and corresponding BJH pore size distribution curve (inset) and (b) XRD patterns for meso−macroporous alumina (TBOA, pH 7).

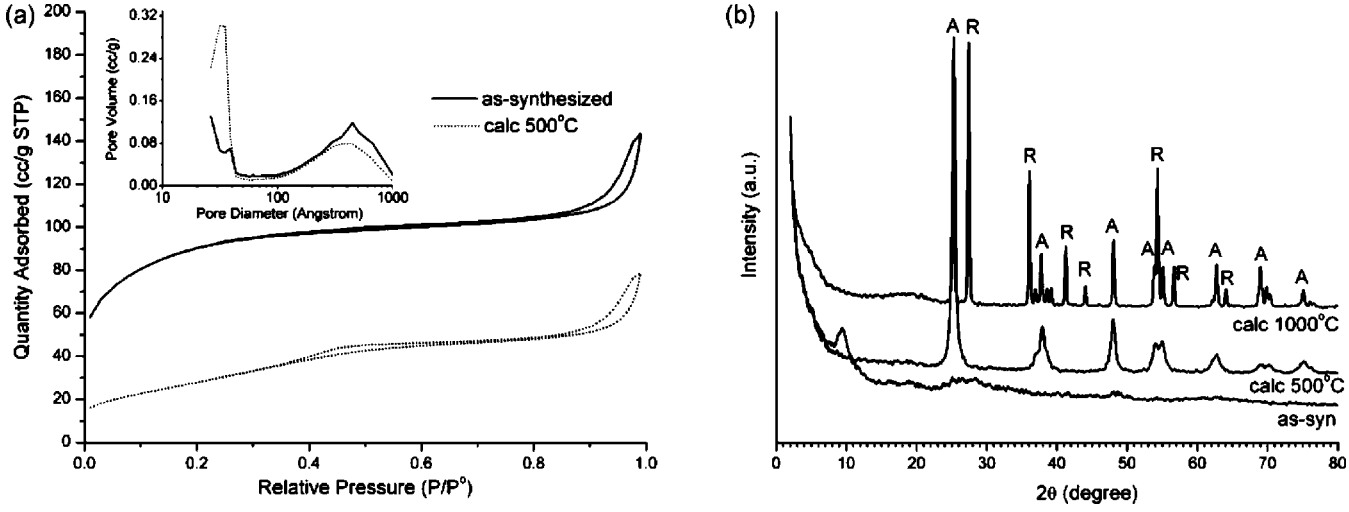

Figure 2. (a) N_2 adsorption−desorption isotherm and corresponding BJH pore size distribution curve (inset). (b) XRD patterns for micro/meso−macroporous titania (Ti isopropoxide, pH 7) (A = anatase, R = rutile).

The total surface area reduced to 136 m^2/g after calcination at 500 °C and to 8 m^2/g after 1000 °C.

XRD patterns of the alumina particles indicated the presence of mixed boehmite and bayerite phases (Figure 1b). The boehmite phase became more pronounced with increasing aging time and temperature. This observation was consistent with mesoporous materials resulting from the assembly of nanoparticles.[22] The as-synthesized titania materials were amorphous. Heat treatment transformed the channel walls into anatase after calcination at 500 °C and into a mixture of anatase and rutile after calcination at 1000 °C (Figure 2b). As-synthesized zirconia materials were amorphous, and no phase was detected after aging or after calcination at 1000 °C (Figure 3b). The formation of crystalline phases did not influence the formation of macropores but did change the mesostructures of the materials.

3.2. Effect of Alkyl Groups and pH. The effect of the alkyl group on morphology was best studied for titanium oxide materials because of the readily available variety of liquid titanium alkoxides allowing investigation of alkyl chain length as well as degree of branching, both of which are important sol−gel parameters.[23,31] The morphology of the final materials from most alkoxide precursors considered here gave a strong dependence on the pH of the reaction mixture. Highly acidic conditions such as pH 0.5 resulted in a clear solution due to the inhibition of the polycondensation process. The structural properties in the final aluminas were very similar for pH 2 and 3. However, pH values lower than 2 resulted in a gelatinous alumina precipitate. Therefore, a pH value of 3 was selected as the lower limit for the comparison study.

SEM analysis revealed different extents of macroporosity in the final powders obtained using various titanium alkoxide precursors. When the syntheses were performed under acidic conditions (pH 3), the highest extent of macroporosity was observed for isopropoxide and *tert*-butoxide precursors, while

(31) Livage, J.; Henry, M.; Jolivet, J. P.; Sanchez, C. *MRS Bull.* **1990**, *15*, 18–25.

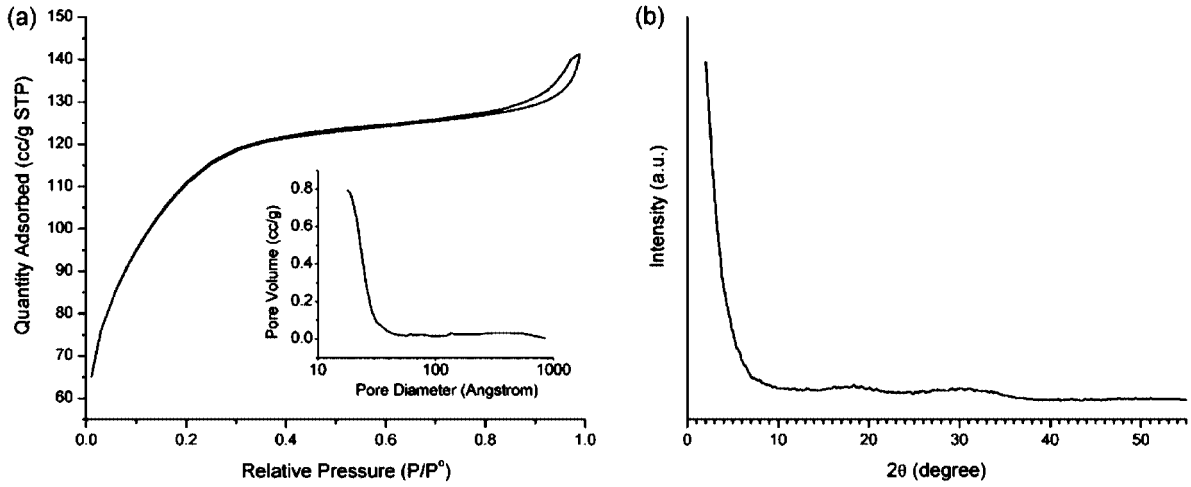

Figure 3. (a) N_2 adsorption−desorption isotherm and corresponding BJH pore size distribution curve (inset). (b) XRD pattern for micro/meso−macroporous zirconia (Zr butoxide, pH 7, aged).

ethoxide, *n*-propoxide, and *n*-butoxide alkoxides produced powders with limited and localized macroporosity with irregularities and wide pore size distributions (Figure 4). Under these conditions, although the powders obtained with titanium isopropoxide had higher extents of macroporosity, the macropore structure appeared disordered. The macropores in the powders obtained using titanium *tert*-butoxide were smaller in size (∼2.0−2.5 μm compared to 3.5−4.5 μm for powders obtained using isopropoxide; Table 1), abundant, and appeared to have a higher structural order relative to macropores in powders obtained using other titanium alkoxides. The morphology and pore structure in the final metal oxide obtained using titanium *n*-butoxide, as seen from the figure, are very different than powders obtained using other alkoxides. These particles have broad shallow pores with a wide size distribution and smooth walls between the pores.

When the pH was increased from 3 to 7, the effect on macroporosity was unsubstantial. However, on further increasing the pH to 11.5, a tremendous increase in order and macroporosity was observed for titanium ethoxide (∼5 μm) and titanium *n*-propoxide (∼7 μm). The extent and order also appeared to improve for titanium isopropoxide (∼4.5 μm). These results were in agreement with those obtained by Collins et al., where they observed that lowering the concentration of ammonia retarded the rate of condensation, which reduced the extent of macroporosity.[15] However, for titanium *tert*-butoxide, less abundant and localized macropores were observed. Powders obtained with titanium *n*-butoxide also displayed some increased levels of porosity at this pH. This pH could be considered as an optimum pH for obtaining macroporosity in titanium oxides and also the pH where the difference between the powders obtained using different alkoxides was least significant (Figure 5).

When the pH was further increased to a more alkaline value of 13.5, the order and extent of macroporosity increased tremendously for titanium *n*-butoxide (∼2.5 μm) but decreased for all other alkoxides. A comparison with titanium *n*-propoxide is presented in Figure 6.

For zirconia materials, the powders synthesized under acidic conditions (pH 3) were found to contain macropores

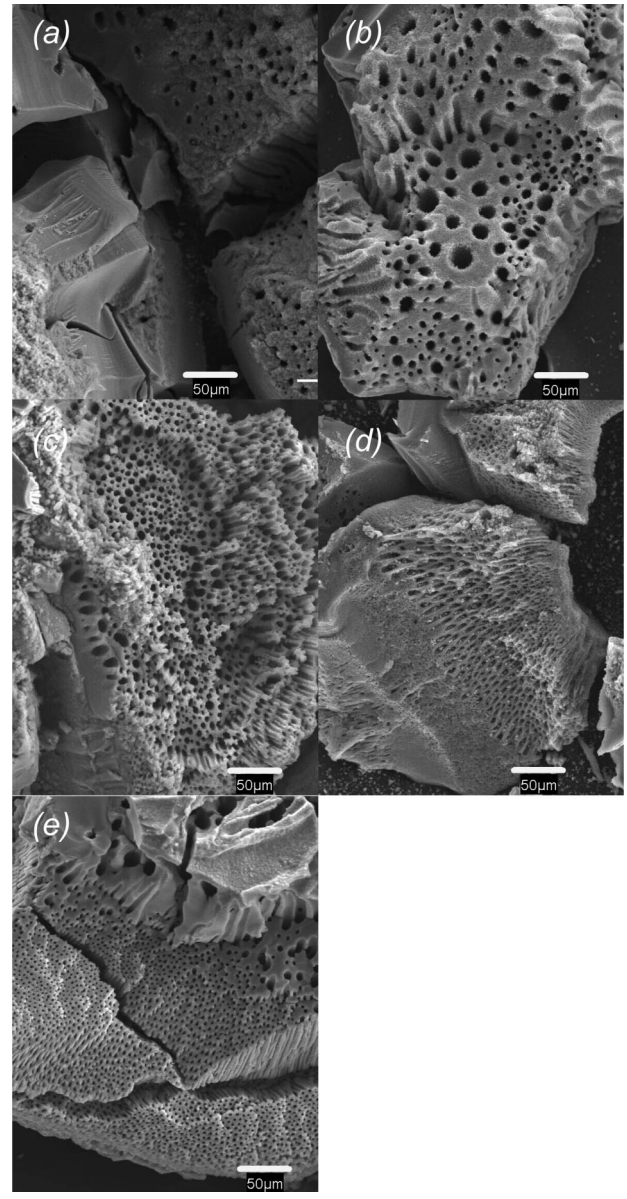

Figure 4. SEM images (500×) of titanium oxide materials synthesized at pH 3 using (a) $Ti(OEt)_4$, (b) $Ti(OPr^n)_4$, (c) $Ti(OPr^i)_4$, (d) $Ti(OBu^n)_4$, (e) $Ti(OBu^t)_4$; scale bar = 50 μm.

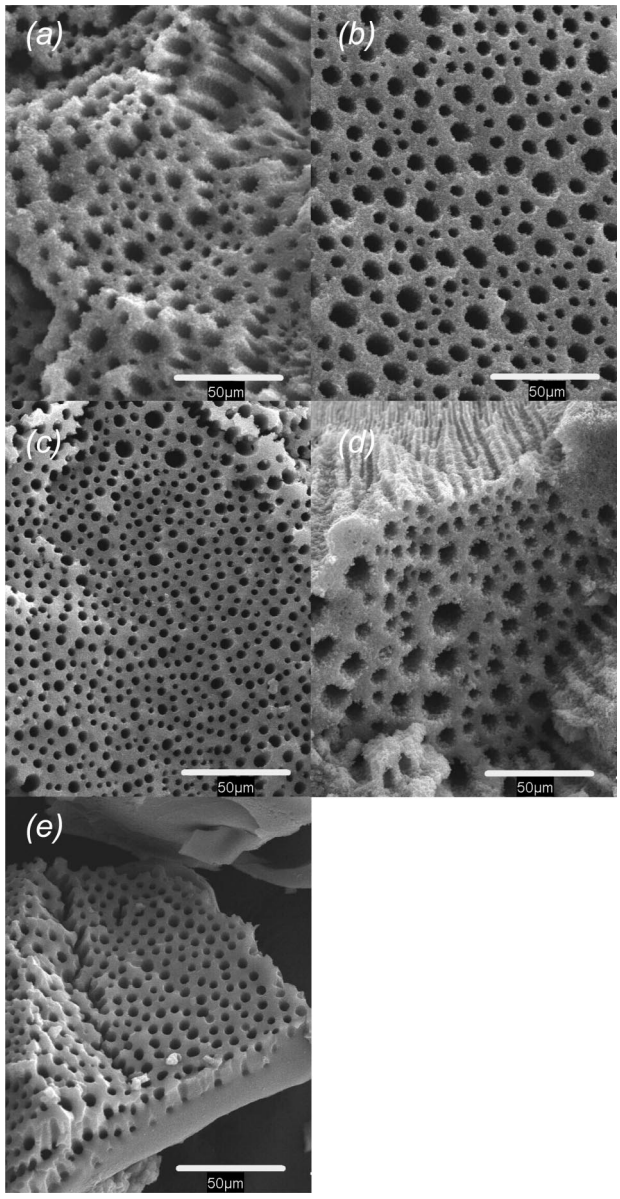

Figure 5. SEM images (500×) of titanium oxide materials synthesized at pH 11.5 using (a) $Ti(OEt)_4$, (b) $Ti(OPr^n)_4$, (c) $Ti(OPr^i)_4$, (d) $Ti(OBu^n)_4$, (e) $Ti(OBu^t)_4$; scale bar = 50 μm.

that were confined to a small portion of the powder particles, while large portions in the particles did not exhibit macroporosity. These limited macropore regions were observed to be more ordered when the starting material was zirconium *n*-propoxide rather than *n*-butoxide. For the case of zirconium *n*-butoxide, a greater number of particles were macroporous comparatively but had higher irregularities in structure. No significant influence on the macroporosity was observed when the pH was raised to 7 or to an alkaline value of 11.5. However, a further increase in pH to 13.5 significantly improved the macroporosity in zirconia materials obtained using either of the two zirconium alkoxides (Figure 7). As can be seen from the figure, zirconium *n*-butoxide produced powders with larger macropores (~2.5−5.5 μm) then those obtained using zirconium propoxide (~1.2−2.0 μm).

In contrast, a decrease in the quantity and order of macropores was observed with an increase in pH for the powders obtained using the less reactive aluminum tri-*sec*-butoxide (Figure 8). The results were in agreement with earlier work where boehmite powders synthesized at acidic

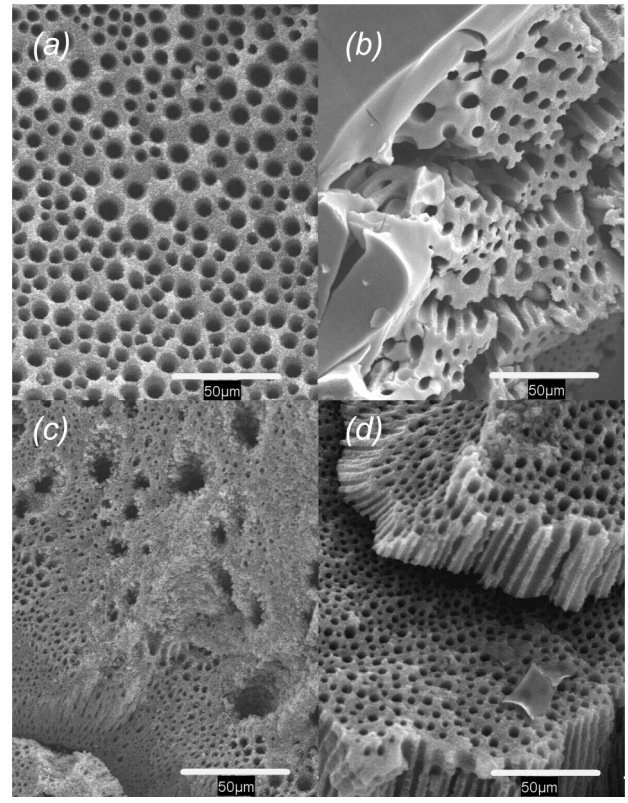

Figure 6. SEM images (500×) of titanium oxide materials synthesized using $Ti(OPr^n)_4$ at (a) pH 11.5 and (b) pH 13.5 and using $Ti(OBu^n)_4$ at (c) pH 11.5 and (d) pH 13.5; scale bar = 50 μm.

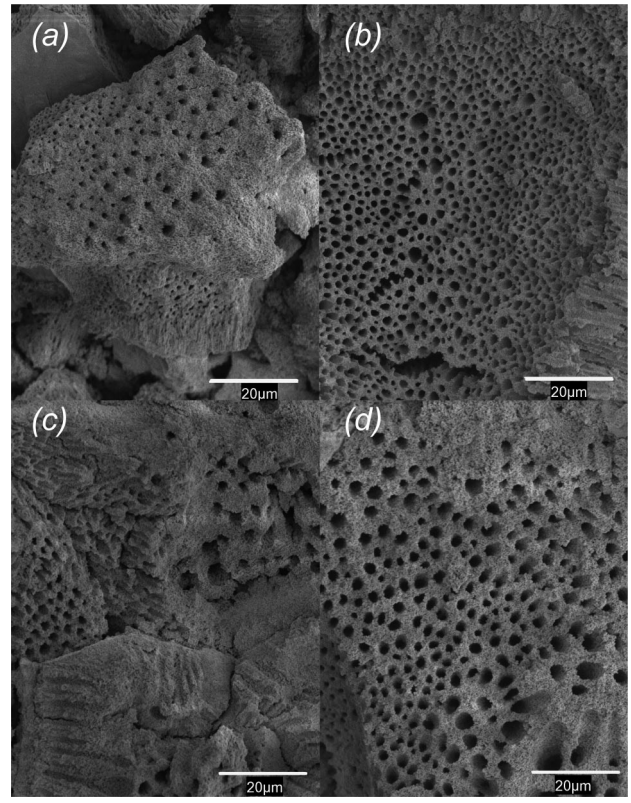

Figure 7. SEM images (1000×) of zirconium oxide materials synthesized using $Zr(OPr^n)_4$ at (a) pH 3 and (b) pH 13.5 and using $Zr(OBu^n)_4$ at (c) pH 3 and (d) pH 13.5; scale bar = 20 μm.

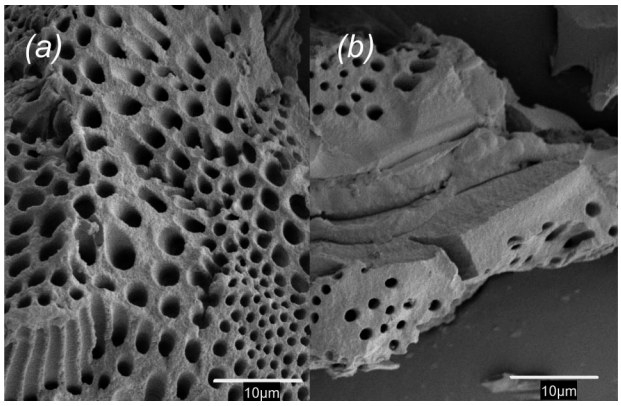

Figure 8. SEM images (2000×) of aluminum oxide materials synthesized at (a) pH 3 and (b) pH 13.5; scale bar = 10 μm.

pH were found to contain a higher population of macropores relative to those obtained under higher pH conditions.[8] The effect of pH was observed not only in terms of the extent of porosity but also in terms of pore size (Table 1). Macropore size in boehmite powders appeared to be smaller (1.2−1.5 μm) for higher pH syntheses as compared to the syntheses performed at acidic or neutral pH (2.5 μm).

Hg porosimetry was performed to complement the results from SEM analysis. A representative Hg-intrusion curve for alumina (pH 3 synthesis) is shown in Figure 9a. The region from 300 to 200 μm corresponds to only powder compaction. The region from 200 to 20 μm represents linear intrusion into the interparticle void spaces. A plateau was reached in the region from 20 to 4 μm, which was followed by a second linear increase in the region from 4 to 0.4 μm due to intraparticle intrusion into the macropores. A plateau in the region from 0.4 to 0.02 μm indicated no more intrusion.

The intrusion plots for the titania samples were more difficult to interpret due to the complex morphology as observed by SEM, which consisted of the macropores as well as distinct particles in the pore walls that gave interparticle pores. As a result, a linear intrusion was observed for the entire plot and a discrete peak for macropores was not be obtained. The pore size distribution plot in Figure 9b shows differences in the 2−4 μm pore diameter region between the titania materials obtained under alkaline conditions (macroporous) and neutral conditions (macropore free). The sample prepared under neutral conditions contained either no or a very small number of macropores; however, a large number of macropores were present in the powder synthesized under alkaline conditions (pH 11.5). A similar intrusion behavior was expected for the zirconia materials, since they had interparticle pores similar to the titania samples.

3.3. Discussion. The results clearly demonstrate that the pattern formation can be greatly influenced by carefully controlling the fundamental chemistry that takes place in the initial stages in the solution by means of adjusting the sol−gel parameters. As mentioned earlier, we have assumed sol−gel-type chemistry to be applicable for the spontaneous self-assembly process; hence, an appropriate starting point is to provide the basics of the sol−gel chemistry of the various materials considered in the current work for use in interpreting the observations in this study.

The starting metal alkoxides are very reactive in aqueous solutions and readily form hydrous oxides,[31] as shown in (1).

$$M(OR)_n + nH_2O \rightleftharpoons M(OH)_n + nROH \quad (1)$$

Two chemical processes, hydrolysis and condensation, are involved in the formation of an oxide network from alkoxides via inorganic polymerization reactions. The first step is hydrolysis of the alkoxide, which occurs upon the addition of the alkoxide to an aqueous solution (2).[23]

$$M{-}OR + H_2O \rightleftharpoons M{-}OH + R{-}OH \quad (2)$$

As a result of this reaction, a reactive hydroxo group (M−OH) is generated. As soon as the first alkoxy (−OR) group in the alkoxide $M(OR)_n$ is substituted by −OH, condensation can occur. It is a very complex process, and depending on the reaction conditions, one or the other of the following is applicable.[31] Olation leads to the formation of OH bridges (3). This occurs when the full coordination of the metal atom is not satisfied in the alkoxide ($N - z \neq 0$; where N is the coordination number of the central metal atom and z is the oxidation state) and the reaction rate is usually very fast.

$$M{-}OH + M{-}XOH \rightarrow M{-}OH{-}M + XOH \quad (X = H \text{ or alkyl group}) \quad (3)$$

Oxolation (elimination of water) and alcoxolation (elimination of alcohol) leads to the formation of oxygen bridges (4). These are relatively slower processes and follow a mechanism similar to that of hydrolysis.

$$M{-}OH + M{-}OX \rightarrow M{-}O{-}M + XOH \quad (X = H \text{ or alkyl group}) \quad (4)$$

It has been demonstrated extensively in the literature that the chemistry taking place in the early stages of the process significantly determines the subsequent processes and the main properties of the synthesized gels.[25,26] The relative contributions of these reactions determine the structure and morphology of the resulting oxides (Table 2).[23] The contributions can be optimized by carefully adjusting the synthesis conditions relative to various parameters, such as the central metal atom of the alkoxide, the alkyl group in the alkoxide, hydrolysis ratio, pH, and temperature of the solution.[13,23,24]

Macroporous powders were obtained under the conditions shown in the third row of Table 2, when both of the reactions were rapid. For sol−gel processes, it has been demonstrated that the chemistry controlling the resultant particle size and morphology often occurs within 1 s.[26] The condensation process is relatively as fast as the rapid hydrolysis of the reactive alkoxides.[25,26,32] The rate is comparable, even in the presence of reaction inhibitors such as acids and complexation ligands.[25] The reactions proceed even faster for spontaneous self-assembly of macroporous materials, where the rates are not inhibited as in sol−gel processes. Additionally, the syntheses were performed in excess water, which led to almost instantaneous precipitation of the final metal oxide particles.

Among the sol−gel parameters mentioned, the ones that were found to affect the formation of macropores in the

(32) Harris, M. T.; Singhal, A.; Look, J. L.; Smith-Kristensen, J. R.; Lin, J. S.; Toth, L. M. *J. Sol-Gel Sci. Technol.* **1997**, *8*, 41–47.

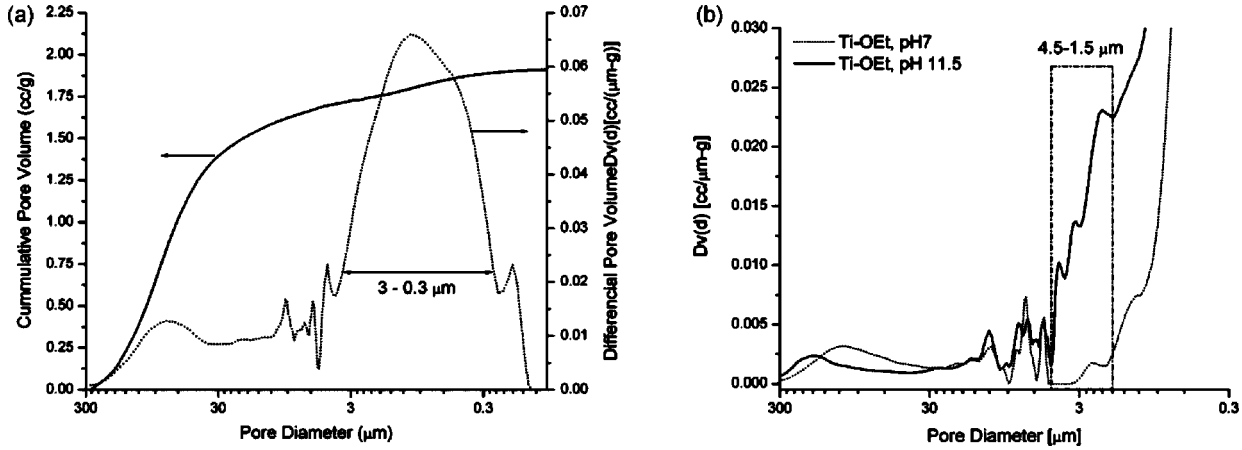

Figure 9. (a) Hg-intrusion curve and corresponding pore size distribution for alumina (pH 3). (b) Pore size distribution from mercury intrusion for titania.

Table 2. Products Obtained Depending on the Relative Rates of Hydrolysis and Condensation

hydrolysis rate	condensation rate	result
slow	slow	colloids/ sols
fast	slow	polymeric gels
fast	fast	colloidal gel or gelatinous precipitate
slow	fast	controlled precipitation

resultant precipitates were the central metal atom in the alkoxide, the alkyl group, and the pH of the solution. Having a highly electropositive central metal atom was crucial, as these patterns were not obtained when less reactive silicon alkoxides were used as starting materials.[8] The transition metal alkoxides are most reactive because of their high electropositivity and their ability to readily expand their coordination number upon hydrolysis. Zirconium is the most electropositive of the metals considered in this work and it has the most rapid hydrolysis rate.[26] The reactivity order is zirconium > titanium > aluminum. Unlike with our self-assembly process, structures from reactive transition metal alkoxides were somewhat difficult to obtain using either sol−gel or phase separation processes, because their high reactivity toward hydrolysis makes control of the structural development difficult until gelation.[4]

Whether or not the macroporous structure will be obtained is determined by the reactivity of the alkoxide central metal atom; however, a finer adjustment of the macroporous pattern in a particular material can be achieved by an appropriate choice of the alkyl group comprising the alkoxide. The size and structure of the alkoxide group strongly influence the rate of hydrolysis.[25] In general, the larger the alkyl group, the slower and less complete is the hydrolysis.[33] The positive partial charge on the central metal atom decreases due to the inductive (electron releasing, +I) effect of the alkyl group, which increases with an increasing number of carbon atoms. The slower hydrolysis of titanium *n*-alkoxides with an increase in the size of the alkyl group has been confirmed.[23] For isomeric alkoxides, the hydrolysis rate trend is tertiary (tert) > secondary (sec) > normal (n) in general, as demonstrated for titanium butoxide, for which the rate decreases as the branching decreases.[25] Combining these observations, the hydrolysis rate for the various alkoxides, considered in the current work, would be expected to follow the trends

$$Ti(OEt)_4 > Ti(OPr^i)_4 > Ti(OPr^n)_4 > Ti(OBu^t)_4 > Ti(OBu^n)_4$$

and

$$Zr(OPr^n)_4 > Zr(OBu^n)_4$$

Harris and co-workers observed that zirconium butoxide hydrolyzes rapidly and more extensively than titanium ethoxide.[32] This result helps to define the relative positions for these two alkoxides in the above ordering. Additionally, with aluminum being the least electropositive metal atom, the overall hydrolysis rate order for the alkoxides use in this study is expected to be

$$Zr(OPr^n)_4 > Zr(OBu^n)_4 > Ti(OEt)_4 > Ti(OPr^i)_4 > Ti(OPr^n)_4 > Ti(OBu^t)_4 > Ti(OBu^n)_4 > Al(OBu^s)_4$$

While the hydrolysis process is well-studied, relatively little exploration has been made toward the condensation phenomenon, which is very complex and might occur in a number of possible paths, as mentioned earlier. One of the few known properties is that, similar to hydrolysis, the low coordination number of the metal atom in nonhydrolyzed transition metal alkoxides is also correlated with their high rates of condensation.[23] Moreover, it has been demonstrated that the condensation process also depends on the size of the alkyl group in the alkoxide (−OR). For example, slower condensation rates were found to be associated with larger alkyl groups in titanium alkoxides.[23] It was observed that the precipitates were formed very quickly in the case of ethoxide (−OEt) and isopropoxide (−OPr^i), while it took significantly longer for *n*-butoxide (−OBu^n).[25] However, a definitive trend for condensation rates is not available in the literature as it is for hydrolysis rates.

The importance of the alkyl group in the determination of the final morphology of the materials obtained by a spontaneous self-assembly route has been demonstrated by

(33) Bradley, D. C. *Adv. Chem. Ser.* **1959**, *23*, 10–36.

a number of researchers. Yoldas observed that the type of alkyl group strongly affected the particle size and morphology of their synthesized zirconium oxides.[24] The macroporosity in the titania powders obtained by Collins et al. was observed to be a function of the starting alkoxides.[15] In a study performed by Ren and co-workers,[18] a bimodal morphology could be obtained only by using titanium *tert*-butoxide as the alkoxide precursor and could not be obtained with any other titanium alkoxide precursor.

In sol−gel chemistry, it was found that particle morphology strongly depends upon the molecular structure of the alkoxy groups as well. The difference in molecular structure of these groups leads to different behavior toward hydrolysis and condensation.[31] In general, alkoxides with primary alkoxy groups associate to form trimers, while those with secondary and tertiary alkoxy groups remain monomeric. In contrast to oligomeric titanium ethoxide and *n*-butoxide in their pure liquid state, isopropoxide and *tert*-butoxide are monomeric and more reactive, because titanium has only a coordination number of four and is attracted to nucleophilic species to expand its coordination sphere. In the hydrolysis experiments performed in the respective parent alcohols, it was observed that for titanium isopropoxide condensation occurred as soon as the hydrolyzed species began forming. The simultaneous occurrence of comparably fast hydrolysis and condensation led to polydispersed species formation.[25] Slower hydrolysis of oligomeric titanium ethoxide relative to condensation, however, led to monodispersed species formation under similar conditions.[31] Thus, oligomerization provides a very convenient way to slow down hydrolysis, thereby adjusting the contribution of hydrolysis and condensation.[31]

Apart from the internal parameters discussed above, an important external parameter for regulating the relative contributions of hydrolysis and condensation reactions is the pH of the solution. In an acidic medium, rapid protonation of the negatively charged −OR groups leads to fast hydrolysis (5).[25]

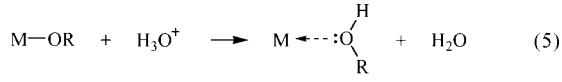

(5)

This result has been established as a general conclusion for all alkoxides.[23] In the presence of an acid, the hydroxo groups are preferentially generated at the end of the chains, giving rise to linear polymers and hence open structures.[23] However, addition of acid slows down the condensation process considerably.[13]

In contrast, a strong base can behave as an inhibitor to the hydrolysis of the metal alkoxide.[26] The presence of a strong base can lead to nucleophilic addition of −OH, decreasing the positive charge of the metal atom. In a basic medium, the condensation process is activated.[25] A highly nucleophilic species $M-O^-$ is formed in the presence of a base such as sodium hydroxide (NaOH) or ammonia (NH_3) that rapidly attacks the positively charged metal, resulting in the formation of strongly cross-linked polymers (6).

(6)

As a result of these apposing effects, acid and base catalysts can be used to promote decoupling between the hydrolysis and condensation reactions. In a very acidic medium, hydrolysis is completed before significant condensation can begin. In a neutral or basic medium both reactions take place simultaneously.[31] Therefore, to increase the contribution of hydrolysis, the synthesis is performed in an acidic medium, while a basic medium is used for condensation to proceed faster.

Consideration of a variety of precursor materials collectively in the current study enables association of the complex chemistry with the presence of macropores in the final materials while drawing conclusions that were difficult to ascertain from previous studies that explored only a portion of the synthesis space that result in macroporous materials. The observations made in the previous section can be organized as follows.

The powders obtained from the titanium alkoxides at either pH 3 or 7 had limited regions of macroporosity in general. However, the macroporosity increased significantly in the powders obtained from almost all of the titanium alkoxides when the starting solution pH was increased to an alkaline value of 11.5. A further increase in pH to a value of 13.5 led to a decrease in macroporosity in powders from all but titanium *n*-butoxide.

When the more reactive zirconium alkoxides underwent hydrolysis/condensation at a pH value of 3, powders with limited regions of macroporosity were obtained. No significant change relative to the macroporosity was observed when the pH was increased to either a neutral or an alkaline value of 11.5. However, the powders obtained at pH 13.5 were highly macroporous.

The powders obtained from the less reactive aluminum alkoxide under acidic or neutral pH had higher extents of macroporosity than the powders obtained under alkaline conditions. An increase in pH to alkaline values with this alkoxide led to a decline in the macroporosity in the resulting alumina powder.

Taken together, very consistent behavior was found for this range of alkoxide species with the observation explainable in terms of hydrolytic condensation phenomena. While a rapid hydrolysis process is required for the formation of macropores, the rapid rate of the condensation process is equally important. A faster hydrolyzing aluminum tri-*sec*-butoxide did produce macropores over a wide range of pH values; however, the highest extent of macroporosity was observed under acidic conditions, where the hydrolysis process is favored. This can be attributed to the reactivity of aluminum alkoxide toward hydrolysis, which is faster than with silicon alkoxides (which did not produce pattern) but slower relative to the transition metal alkoxides. For aluminum alkoxide, hydrolysis rate enhancement is required to produce the macroporous structure. In contrast, titanium alkoxides hydrolyze much faster, and because of the very dominant hydrolysis process, the macropattern in the final powders was either very poor or absent. When the condensation process was enhanced by performing the syntheses at pH 11.5, it resulted in powders with significantly increased extents of macroporosity. A further increase in the condensa-

tion rate by performing the synthesis at a higher pH value of 13.5 was actually found to be detrimental to the structure formation. This result was possibly due to slowing down the hydrolysis process due to the presence of a large number of hydroxyl groups, leading to their nucleophilic addition to the central metal atom. However, in the fastest hydrolyzing zirconium alkoxides, a high pH value of 13.5 was necessary to enhance the condensation process relative to hydrolysis in order to obtain powders with improved macroporous structure. In the case of the aluminum alkoxide, the increase in pH to favor the condensation process resulted in powders that appeared to have lesser extents of macroporosity, possibly due to the slowing down of the aluminum alkoxide hydrolysis rate, which already is less reactive than the transition metal alkoxides.

Therefore, independently optimizing the synthesis conditions in favor of either hydrolysis or condensation was not sufficient. Instead, the results suggested that there was an optimum window for balancing the contributions from both hydrolysis and condensation, which favored the formation of macropores; this region could be achieved by adjusting the relative rates of these two reactions. For titanium alkoxides with intermediate hydrolysis rates, this window could be approached by enhancing the condensation process relative to hydrolysis when the pH value was increased to 11.5. For more reactive zirconium alkoxides, a higher pH value of 13.5 was required for obtaining the desired balance. The balance was not achieved when the pH was increased for the aluminum alkoxide, which already had comparatively insufficient hydrolysis rates that were further exacerbated under basic conditions. The balance was realized for the aluminum alkoxide under acidic conditions. The one alkoxide that did not respond as expected to the synthesis pH was titanium *n*-butoxide, which although being the least reactive of all titanium alkoxides, still produced the best macroporous product at a pH of 13.5.

The improved formation of macropores with titanium isopropoxide and *tert*-butoxide at the lower pH value can be understood by considering the molecular structure of these metal alkoxides. As discussed previously, the steric hindrance from the branched alkyl groups in these alkoxides screens the central metal atom and prevents the formation of dimers and trimers to satisfy the unsaturated coordination number. Consequently, these alkoxides are monomeric in their pure form, which renders them very reactive due to unsaturated coordination, and their hydrolyzed species condense quite rapidly, which would be favorable for creation of the desired morphologies.

The behavior of the different alkoxide precursors in response to pH variation provides some insight into previous literature reports.[20] As demonstrated in the current study, the alkoxides of different materials have different optimum pH values for forming these structures. Zirconium alkoxides yielded powders with similar macroporous structure over a wide pH range and a significant improvement was observed only after increasing the pH value to 13.5. The aluminum alkoxide also produced powders with a high extent of macroporosity over a wide range, but high alkalinity led to deterioration in the macroporosity. In contrast, most of the titanium alkoxides produced powders with the desired macroporous structure only for pH values near 11.5. Therefore, titania materials are more sensitive to changes in pH. It appeared that the necessary balance between hydrolysis and condensation could be maintained for a larger pH range with alumina materials than with titania materials, which is why macroporous powders were obtained by the Su group over a wider range for alumina or aluminosilicates[20] than for titania. Collins and co-workers associated smaller macropore size and more ordered structure with a slower hydrolyzing titanium alkoxide. However, in our experiments, we did not observe a consistent trend in the macropore sizes with the hydrolysis rates of the titanium alkoxides. Additionally, zirconium butoxide, which hydrolyzes more slowly than zirconium propoxide, produced powders having macropores with almost twice the size under similar conditions. With the exception of zirconium butoxide, a specific alkoxide precursor did appear to produce smaller macropores for a higher starting pH value of the synthesis solution (Table 1).

Collins et al.[11] proposed a mechanism for the macropore formation in which an outer semipermeable shell is formed instantaneously after the introduction of an alkoxide droplet into the synthesis solution with the reaction front proceeding inward. Inside the shell encased droplet, the hydrolysis and condensation were proposed to proceed in concert in such a way as to rapidly produce solid nanoparticles and liquid byproducts, which leads to the formation of microseparated domains that gave rise to the macropore structure. The indispensable need for the rapidity of the process has been highlighted in terms of rapid polymerization.[10] Collins et al. also speculated that rates of hydrolysis/condensation and/or the nature of alcohol byproducts are important in determining the final morphology. The current study demonstrated how this rapid polymerization process is a product of the balance between the constituent hydrolysis and condensation reactions, signifying the importance of both acting in a concerted manner. When the balance between these two reactions was maintained, the proposed mechanism of rapid production of solid and liquid phases could be attained. Unlike aluminum and transition metal alkoxides, silicon alkoxides are not as reactive with water, thus not satisfying the indispensable need of a rapid hydrolysis/condensation process to yield macroporous materials. The attempts to obtain similar patterns using tetramethoxysilane and tetraethoxysilane were made, but the syntheses led to the formation of uniform spherical particles of 200 nm diameter and no macropores.[8]

We found that observing the behavior of the different alkoxides upon introduction to the aqueous medium could provide insight into whether macropores were formed. With the titanium alkoxides, the materials were characterized by a faster transition of the immiscible alkoxide droplets in the synthesis solution to an opaque white solid. These solid particles retained the shape of the original droplets apart from the development of cracks on the surface due to stress. When carefully observed under SEM, these were found to consist of a smooth outer shell and a highly macroporous inner region (Figure 10). Due to their fragile nature, the powder particles were fragments of these bigger particles and great care was taken while imaging to investigate the individual

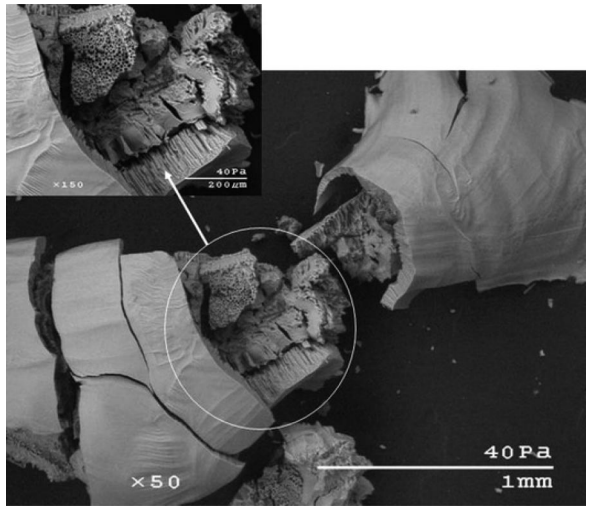

Figure 10. SEM image of titanium oxide particle with outer shell and inner macroporous structure.

particles for regions of macroporosity and regions that were macropore free. Such a transition was almost instantaneous for titanium alkoxides in the pH 11.5 solution and was complete in a few seconds, while the process was considerably slower under acidic pH, where transparent beads slowly transformed to white solids. At a pH of 13.5, the alkoxide spread upon introduction to the aqueous solution, and the final powder had particles with a low quantity of disordered macropores. For zirconium, the transformation to a white solid, while retaining the shape of droplets, was fastest at a pH of 13.5 and, similar to titanium alkoxides, was completed in a matter of seconds. These materials were observed to be highly macroporous. Conversely, for the aluminum alkoxide, which under acidic and neutral conditions took several minutes to transform completely into a solid particle suspension, an increase in pH resulted in longer times for the transformation, and the observations revealed that these powders had lower levels of macroporosity. The observations seem to be consistent with the proposed model, but questions regarding the true mechanism of pore initiation and microphase separation and whether the diffusion of water through the resistance of the outer mesoporous shell and against the counter diffusion of alcohol species is sufficiently fast to match the rapid hydrolysis at the water−alkoxide interface require further investigation.

4. Conclusion

Macroporous structures for aluminum oxyhydroxide, titanium oxides, and zirconium oxides were systematically obtained starting from different alkoxide precursors via spontaneous self-assembly in an aqueous medium. The unified synthesis approach in the current work provided a common basis for comparing a variety of macroporous metal oxides synthesized under similar conditions in a single study. This work provided more uniform comparison of these metal oxides than was provided by various independent studies in the literature. The chemistry of the process was investigated for improved understanding of macropore structure formation by examining the effects of sol−gel parameters such the as alkyl group of the starting alkoxides and the central metal atom as well as pH of the starting solution. The results suggested that the hydrolysis and condensation rates must be within a certain range for these morphologies to occur; however, these processes cannot be viewed independently, as it is the relative rates of these two concerted reactions that dictated the formation of macroporous metal oxides. The synthesis parameters influenced both the extent of the macroporosity and the size of the macropores. For a particular metal oxide, appropriate selection of the precursor alkoxide and solution pH can tune the resulting macropore size. While the work provides a more consistent basis of comparison for the formation of macroporous metal oxides, the precise mechanistic cause of this unique structure formation remains unclear.

Acknowledgment. We acknowledge the financial support from the Petroleum Research Foundation (American Chemical Society).

CM801691G